Structural Model Identification of a Small Flexible Aircraft

Claudia P. Moreno, Abhineet Gupta, Harald Pfifer, Brian Taylor, and Gary J. Balas[1]

Abstract— **The system identification of a light-weight, high-aspect ratio wing is presented. Experimental data is obtained from a ground vibration test. The input signals are sine sweep wave forces and the outputs are the corresponding acceleration responses of the aircraft. Subspace algorithms are used to estimate a state-space model of the aircraft. Minimization of the model prediction error is performed to fit the frequency response data. As result, the estimated model identifies six structural modes between 5 Hz and 30 Hz.**

I. INTRODUCTION

Modern aircraft designers are adopting light-weight, high-aspect ratio flexible wings to improve performance and reduce operation costs. However, the large deformation exhibited by these aircraft increase the interaction of the rigid body dynamics and structural vibration modes -usually the first wing bending mode. This interaction, called body freedom flutter, leads to poor handling qualities and may result in dynamic instability. Hence, accurate models are required to predict and control this dangerous phenomenon.

Flutter analysis of aircraft has been widely studied [1], [2], [3], [4], and numerous researchers have addressed aeroelastic modeling for highly flexible aircraft [5], [6], [7], [8]. Currently, modeling aeroelastic behavior of flexible aircraft requires the development of a structural model coupled with an aerodynamic model. The nonlinear aeroelastic models are derived based on structural finite elements and lifting-surface theory, both of which are available in general purpose commercial code [9], [10], [11]. However, accurate flutter prediction is highly dependent on the accuracy of these aerodynamic and structural models.

It is standard practice to improve the accuracy of structural models by updating the parameters in the finite element model using experimental modal data. This paper presents the system identification of a highly flexible unmanned aircraft. Natural frequencies, damping factors and mode shapes of the structure are identified for model updating purposes.

The paper is divided in six sections. Section II describes the estimation methods for system identification of state-space models. Section III presents the test vehicle and experimental setup of the ground vibration test performed to obtain structure modal information. Experimental results and identification of modal parameters are presented in Section IV. Finally, Section V shows the validation of the estimated model, and conclusions are in Section VI.

[1]Claudia P. Moreno, Abhineet Gupta, Harald Pfifer, Brian Taylor and Gary J. Balas are with the Department of Aerospace Engineering and Mechanics, University of Minnesota, Minneapolis, MN 55455, USA. moren148@umn.edu, gupta165@umn.edu, brtaylor@umn.edu, hpfifer@umn.edu, balas@umn.edu

II. BACKGROUND

The system identification objective is to build mathematical models of dynamic systems based on data observations. The construction of these models involves three entities: (i) recorded experimental input-output data, (ii) selection of a mathematical modeling framework, and (iii) choice of system identification algorithms that will yield the best model fitting the observed data [12].

State-space models are selected to describe the structural dynamic system. These mathematical models can accurately describe the linear dynamics and can provide physical insight regarding the system. Because the measurement data is usually sampled for computational applications, discrete time state-space models are better suited for system identification purposes. Moreover, state-space models form the basis for many modern control design methods. Hence, the versatility of state-space models is the reason to select them to describe the structural dynamics of the aircraft.

Discrete time, state-space models for identification and control are described by

$$\mathbf{x}(k+1) = \hat{\mathbf{A}}x(k) + \hat{\mathbf{B}}\mathbf{u}(k) + \mathbf{w}(k), \quad (1)$$

$$\mathbf{y}(k) = \hat{\mathbf{C}}\mathbf{x}(k) + \hat{\mathbf{D}}\mathbf{u}(k) + \mathbf{v}(k) \quad (2)$$

where $\mathbf{u}(k)$ and $\mathbf{y}(k)$ are the input and output vector measurements at time instant k, $\mathbf{x}(k)$ is the state vector and $\mathbf{w}(k)$, $\mathbf{v}(k)$ unmeasurable signals representing the noise in the system. $\hat{\mathbf{A}}$ is the dynamic system matrix, $\hat{\mathbf{B}}$ the input matrix, $\hat{\mathbf{C}}$ the output matrix and $\hat{\mathbf{D}}$ the direct feedthrough term.

Several methods have been proposed in the literature to reproduce the measured data [12], [13]. Subspace identification algorithms, based on system theory and linear algebra concepts, are suitable for state-space model identification. These algorithms use the system Hankel matrix of the system, defined as the product of the observability and controllability Gramians.

One algorithm developed for identification of lightly damped systems is the eigensystem realization algorithm (ERA) [13]. In the ERA, deterministic models (i.e. neglecting noise) are used to compute the state-space model. The algorithm exploits the relationship between the impulse response of the structure and the system dynamics.

The impulse response of the discrete time, state-space model described by (1) and (2) corresponds to

$$\mathbf{y}(0) = \hat{\mathbf{D}}, \quad (3)$$

$$\mathbf{y}(k) = \hat{\mathbf{C}}\hat{\mathbf{A}}^{k-1}\hat{\mathbf{B}} \quad (4)$$

The Hankel matrix of the system is constructed using the

impulse response $\mathbf{y}(k)$:

$$\mathbf{H}(k-1) = \begin{bmatrix} \mathbf{y}(k) & \mathbf{y}(k+1) & \cdots & \mathbf{y}(k+p) \\ \mathbf{y}(k+1) & \ddots & & \vdots \\ \vdots & & \ddots & \vdots \\ \mathbf{y}(k+r) & \cdots & \cdots & \mathbf{y}(k+p+r) \end{bmatrix} \tag{5}$$

where the parameters p and r correspond to the number of columns and rows in the Hankel matrix. For good results, p should be selected to be at least ten times the number of modes to be identified, and r should be selected to be 3-5 times p [13], [14].

The Hankel matrix evaluated for $\mathbf{H}(0)$ has the form

$$\mathbf{H}(0) = \begin{bmatrix} \hat{\mathbf{C}} \\ \hat{\mathbf{C}}\hat{\mathbf{A}} \\ \vdots \\ \hat{\mathbf{C}}\hat{\mathbf{A}}^{k+r} \end{bmatrix} \begin{bmatrix} \hat{\mathbf{B}} & \hat{\mathbf{A}}\hat{\mathbf{B}} & \ldots & \hat{\mathbf{A}}^{k+p}\hat{\mathbf{B}} \end{bmatrix} \tag{6}$$

Performing a singular value decomposition of the Hankel matrix, $\mathbf{H}(0) = \mathbf{U}\Sigma\mathbf{V}^T$, where $\mathbf{U}$ and $\mathbf{V}$ are the left and right singular vectors and Σ a diagonal matrix containing the singular values, allows to find a state-space realization of the system. Condensed matrices Σ_n, $\mathbf{U}_n$, $\mathbf{V}_n$ obtained by elimination of relatively small singular values corresponding to computational modes, are used to find the discrete time, state-space matrices as

$$\hat{\mathbf{A}} = \Sigma_n^{-1/2}\mathbf{U}_n\mathbf{H}(1)\mathbf{V}_n\Sigma_n^{-1/2} \tag{7}$$

$$\hat{\mathbf{B}} = \Sigma_n^{-1/2}\mathbf{V}_n^T[\mathbf{I}\ \mathbf{0}] \tag{8}$$

$$\hat{\mathbf{C}} = [\mathbf{I}\ \mathbf{0}]^T\mathbf{U}_n\Sigma_n^{-1/2} \tag{9}$$

$$\hat{\mathbf{D}} = \mathbf{y}(0) \tag{10}$$

Natural frequencies and damping factors are obtained by converting the eigenvalues of the discrete time state-space model to its continuous time representation.

Because the realization of the system obtained using this subspace approach is not unique and depends on the size of $\mathbf{H}(0)$, the model identification can be refined by minimizing the model prediction error.

Numerical optimization is used to minimize the norm of the prediction error defined as

$$I_N(\mathbf{G}) = \sum_{k=1}^{N} [\mathbf{y}(k) - \mathbf{G}(q)\mathbf{u}(k)]^2 \tag{11}$$

where N is the number of samples and $\mathbf{G}(q)$ is the complex frequency response of the discrete system

$$\mathbf{G}(q) = \hat{\mathbf{C}}\left(q\mathbf{I} - \hat{\mathbf{A}}\right)^{-1}\hat{\mathbf{B}} + \hat{\mathbf{D}} \tag{12}$$

with q as the discrete Laplace variable.

III. EXPERIMENTAL METHOD

The Body Freedom Flutter (BFF) test vehicle has a high-aspect-ratio flying wing planform with a rigid center body (fuselage). The flexible wings are made of segmented foam core (see Fig. 1). The vehicle was developed by the U.S. Air Force Research Laboratory and Lockheed Martin Aeronautics Company, and donated to the University of Minnesota [15]. The objective is to identify the modal parameters of the flexible structure using input-output data obtained from a ground vibration test.

A. Boundary Conditions

The vibration test would ideally occur with the vehicle freely suspended in space. In practice, however, a truly free support is not feasible because the structure needs to be held in some way. This condition can be approximated by supporting the test structure on very flexible springs such that the rigid body modes do not interfere with the flexible modes [16]. The BFF free condition is reproduced using a very flexible spring such that the highest rigid body mode frequency is less than 20% of the fundamental frequency of the aircraft.

Because the fundamental frequency of the structure f_n is approximately 5 Hz, the frequency of the mass-spring system f_r must not exceed 1 Hz. The mass of the aircraft is m =5.44 kg. The maximum stiffness of the spring required to achieve an almost free condition is $k = m(2\pi f_r)^2 = 215$ N/m. A stainless steel spring that can support a maximum load of 11.2 kg with a stiffness of 130 N/m is selected to suspend the aircraft from a rigid frame (Fig. 1).

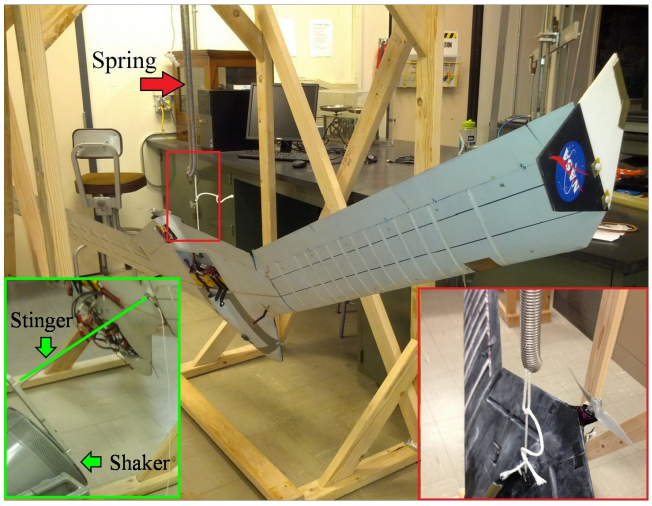

Fig. 1. Test setup: Suspended aircraft with vibration exciter shaker

B. Data Acquisition Equipment

All the equipment used for this experiment is available at the Aeromechanics Laboratory at the University of Minnesota. An Unholtz-Dickie Model 20 electrodynamic shaker is used to provide a known excitation to the structure. The shaker can apply forces up to 1103 N at frequencies between 1-5000 Hz. The structure is connected to the shaker through an excitation stinger. The stinger transmits the excitation force axially and reduces lateral forces applied to the structure.

A PCB 208C01 force sensor is mounted between the stinger and the structure to measure the excitation force. The

sensor can measure forces of ±44.5 N between a frequency range of 0.01-36000 Hz with a sensitivity of 112.41 mV/N. A PCB 353B16 miniature accelerometer is used to measure the structural response at several locations along the aircraft. The measurement range is ±500 g for frequencies from 1 to 10000 Hz. The sensitivity of the sensor is 10 mV/g. In addition, signal conditioners PCB 480E09 are used to amplify voltage gains of the sensors by factors of 1 and 10. Excitation signals and experimental transfer functions between the force applied by the shaker and the acceleration at the different points are calculated using a HP35670A Dynamic Signal Analyzer with 400-data point frequency resolution [17], [18].

C. Experimental Procedure

The aircraft is excited with a sine sweep wave from 3 to 35 Hz. A sampling rate of 70 Hz is chosen by the analyzer to perform the test. This sampling rate allows to determine the structure natural frequencies below 35 Hz. Acceleration responses are measured at 34 points distributed along the wing and center body of the vehicle (Fig. 2). Point 12 was selected as the excitation location. It is expected that vibrations applied in this asymmetric point will excite the symmetric modes and anti-symmetric modes of the structure.

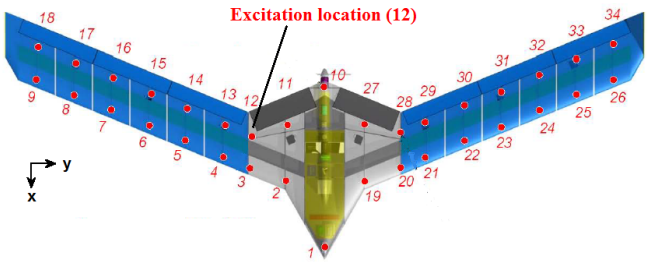

Fig. 2. Input and output measurement locations [15]

Single input, single output (SISO) frequency responses from applied force to acceleration response are obtained at each location using the dynamic analyzer. The frequency responses contain 400 data points and are computed in the swept-sine analyzer mode. Force and acceleration signals are measured at a constant frequency to calculate each point of the frequency response.

An experimental frequency response obtained from the anti-symmetric input to the acceleration response at the tip of the wing is shown in Fig. 3. Peaks in the magnitude response and 180 deg phase changes denote the identification of several modes. In particular the structure has two closely spaced modes between 17 and 20 Hz. These experimental data are used to obtain the modal parameters of the aircraft structure described in the following section.

IV. MODAL IDENTIFICATION

Natural frequencies of the vehicle are determined using the eigensystem realization algorithm (ERA). The impulse response functions required for ERA are computed as the

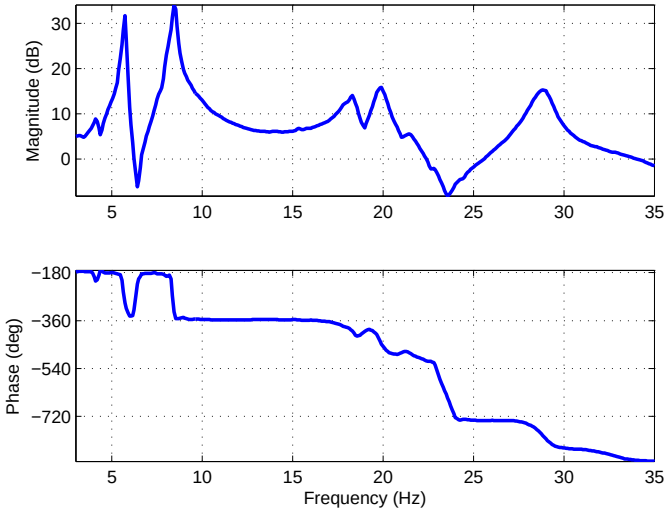

Fig. 3. Experimental frequency response: From force [N] at point 12 to acceleration [g] at point 18

inverse Fourier transform of each experimental frequency response. The Hankel matrix is assembled using 601 samples of the impulse response, corresponding to 500 rows and 100 columns of the matrix.

Individual SISO state-space models with 12 states are estimated for each sensor measurement, leading to 34 models. The order of the systems is selected based on the number of modes to identify. The natural frequencies are determined, and are presented in a scatterplot Fig. 4. Six flexible modes, visualized by the vertical patterns, are identified with these set of measurements. Note that not all of the six modes are identified in each SISO systems. These results probably correspond to measurements located at or very close to the nodes of some modes, where their contribution is very small and as consequence, not seen in the response.

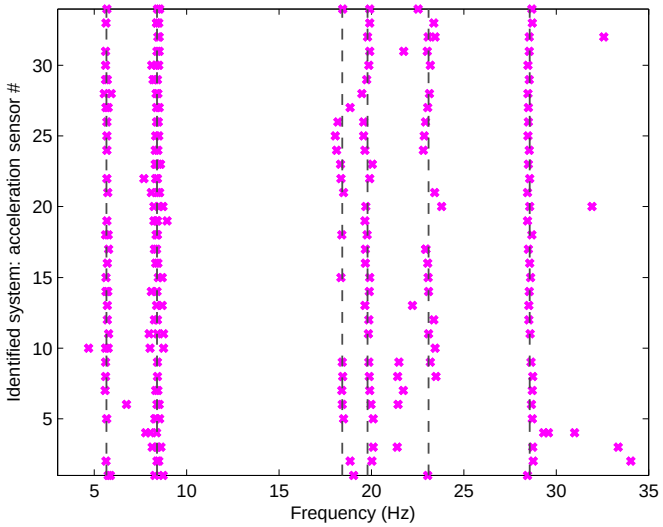

Fig. 4. Identified natural frequencies using ERA

An initial estimate of the natural frequencies of the

structure is obtained by averaging the values corresponding to each identified vertical pattern. The natural frequencies obtained are 5.65, 8.38, 18.41, 19.79, 23.10 and 28.58 Hz as depicted by the dashed line in Fig. 4. Having estimated the modal frequencies, the next step is to find a structural model that reproduces the dynamic behavior of the aircraft at all 34 locations upon excitation at the location 12. This model will be used for tuning and updating of finite element models representing the aircraft structure.

A single input, multiple output structural model is estimated using the MATLAB System Identification Toolbox [19]. A non-iterative subspace approach, combined with numerical optimization of the prediction error, is performed to estimate the model. A state-space model with 20 states was found suitable to capture the six flexible modes initially estimated by ERA. The order of the multiple output model is higher than the order required for the SISO state-space models. This result shows that modeling of multiple output systems is more challenging because input-output couplings require additional parameters to obtain a good fit and involve more complex models [20].

Fig. 5 and Fig. 6 compares the frequency response of the measured experimental data and the estimated state-space system from the force inputs to two acceleration outputs. The estimated model successfully captures the major modal contributions to the system response.

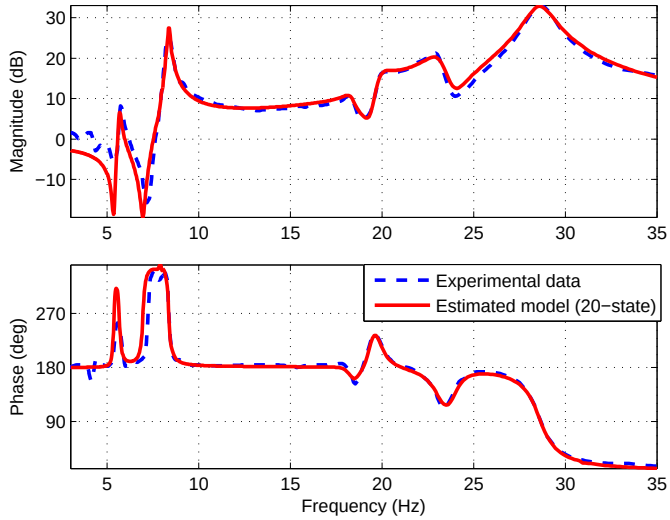

Fig. 5. Frequency response from force [N] at point 12 to acceleration response [g] measured at point 16

Mode shapes of the structure are determined using the quadrature picking technique [21], [22]. In lightly damped structures, the response at a particular natural frequency is completely dominated by the corresponding mode. This implies that the response of the structure is governed by its imaginary part. The relative modal displacement at each point is obtained by evaluating the frequency response function at a particular natural frequency and examining the magnitude and direction of its imaginary part.

Fig. 7 sketches the identified mode shapes and associated

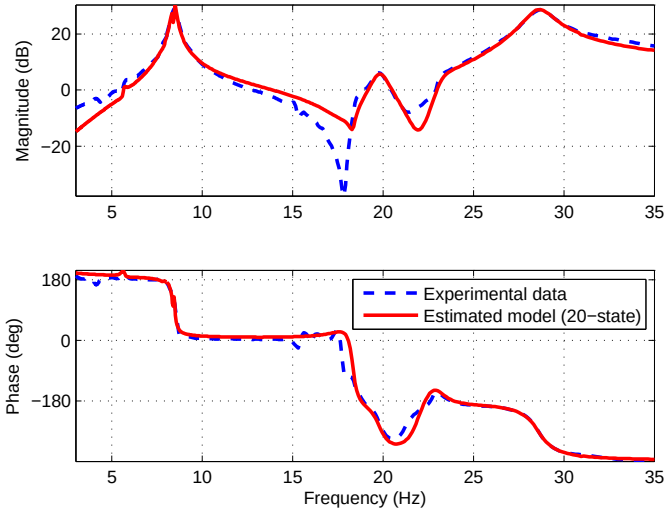

Fig. 6. Frequency response from force [N] at point 12 to acceleration [g] response measured at point 20

natural frequencies of the aircraft. Table I lists the frequency values and damping factors corresponding to the each mode shape identified by the estimated state-space model.

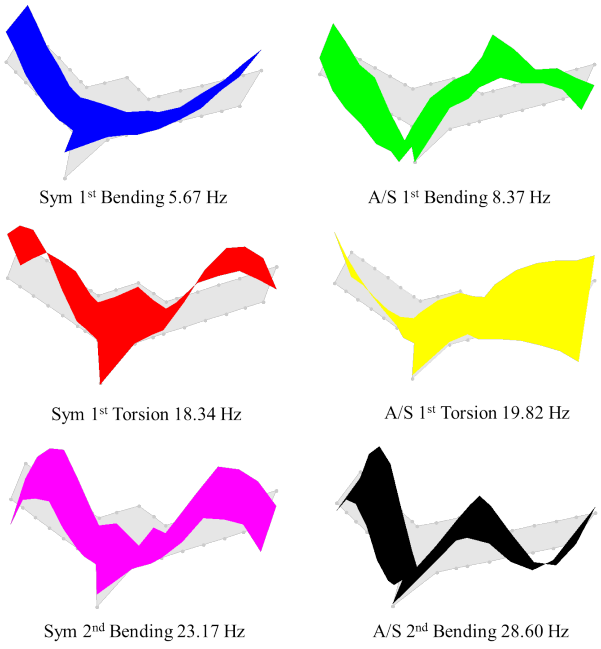

Fig. 7. Identified mode shapes

V. VALIDATION

Model validation is performed using two techniques, the normalized root mean square error (NRMSE) and the ν-gap metric. The evaluation criteria to determine if the estimated model is a good representation of the real system is based on comparing the frequency response predicted by the model and the measured data.

TABLE I

NATURAL FREQUENCIES, DAMPING FACTORS AND MODAL SHAPES

Modal Shape	**Frequency [Hz]**	**Damping [%]**
Symmetric 1st Bending	5.67	1.55
Anti-symmetric 1st Bending	8.37	1.06
Symmetric 1st Torsion	18.34	2.06
Anti-symmetric 1st Torsion	19.82	2.33
Symmetric 2nd Bending	23.17	2.85
Anti-symmetric 2nd Bending	28.60	2.55

The accuracy of the estimated model using the NRMSE is calculated as

$$\%\text{fit} = 100\left(1 - \frac{\|\mathbf{y}-\hat{\mathbf{y}}\|_2}{\|\mathbf{y}-mean(\mathbf{y})\|_2}\right) \tag{13}$$

where $\mathbf{y}$ is the measured frequency response data and $\hat{\mathbf{y}}$ is the predicted frequency response of the model. Here, a value of 100% indicates a perfect fit [20].

Fig. 8 shows the percentage of the input-output frequency response that the estimated model represents. Literature reports five evaluation criteria to categorize the goodness of an estimated model. Fit values $> 70\%$ are excellent models, $> 40\%$ good models and $> 20\%$ poor models [23]. A 70% fit value is chosen to accept the model as a good representation of the aircraft structural dynamics.

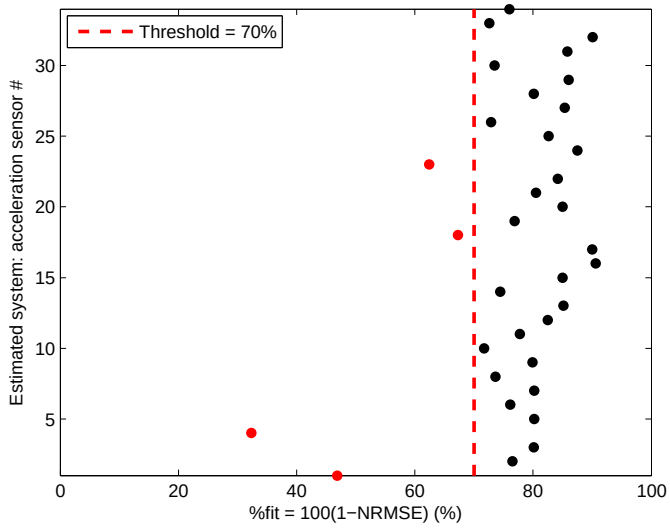

Fig. 8. Percentage of the input-output frequency response represented by the estimated model

It is observed that the estimated model has four input-output frequency responses below the 70% threshold value. This means that the dynamic behavior for those input-output responses is hard to reproduce by the model. This situation can be a consequence of input-output couplings and poor measured data.

Because the model validation using NRMSE is based on the accuracy of each input-output pair, i.e. SISO system, a different metric that evaluates the accuracy of the estimated model in a multiple input, multiple output (MIMO) framework is proposed.

The ν-gap metric is proposed to validate the model in a MIMO framework. This metric provides a measure of the distance between two linear systems in a feedback context. Two systems are considered to be close in the gap metric if, given any stable input-output pair of the first system, there is a corresponding stable input-output pair of the second system that is close to it. The ν-gap metric between two linear systems $P_1(j\omega)$, $P_2(j\omega)$ is calculated in the frequency domain as

$$\delta(P_1,P_2)(j\omega) = (1+P_2P_2^*)^{-\frac{1}{2}}(P_2-P_1)(1+P_1P_1^*)^{-\frac{1}{2}} \tag{14}$$

where $\delta(P_1,P_2)(j\omega)$ lies within the interval [0, 1]. Values close to zero indicate the two systems are identical and values close to 1 that the systems are far apart [24].

Fig. 9 shows the distance between the estimated model and the experimental data over the frequency range of interest, i.e. 5-30 Hz. A ν-gap metric of 0.3 is selected as threshold to determine the goodness of the estimated model. It is observed that the ν-gap metric is below the 0.3 threshold across the frequency range identified. This means that the multiple output estimated model with 20 states is a good representation of the aircraft structural dynamics in the bandwidth of interest.

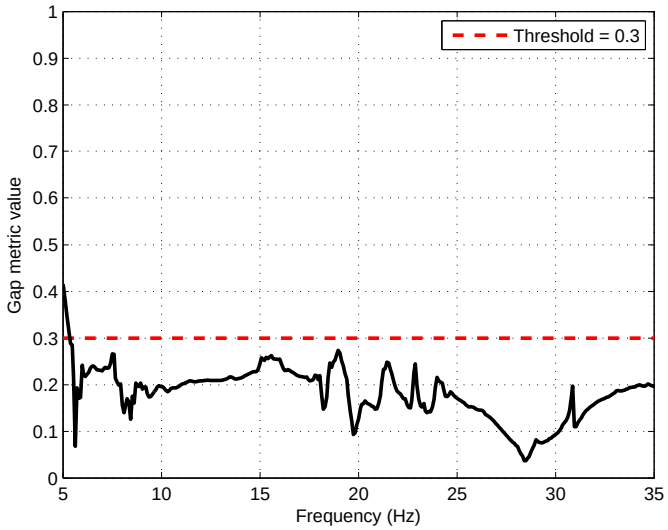

Fig. 9. Distance between estimated model and experimental data across frequency

VI. CONCLUSIONS

A ground vibration test was performed on a flexible unmanned aircraft. Sine sweeps generated by a shaker were used to excite the modal dynamics of the vehicle. The acceleration response to this force excitation was measured at different points along the aircraft. The first six structural modes were successfully identified in the experiment.

Based on the experimental data, a linear model of the structural dynamics that minimizes the prediction error was identified. The model was validated using standard techniques from system identification, namely the normalized root mean square error, as well as techniques from robust

control, i.e. the ν-gap metric. Both validation methods show that the identified model is a good fit of the experimental data.

Future work will incorporate the identified structural model into an overall model of the aircraft, including the aerodynamics and the rigid body modes. The goal is to obtain a high fidelity model of the flexible unmanned aircraft which can be used to design flutter surpression and gust load alleviation controllers.

ACKNOWLEDGMENT

This research is supported by the NASA STTR contract No. NNXIICI09P entitled *Robust Aeroservoelastic Control Utilizing Physics-Based Aerodynamic Sensing* as a subcontract from Tao Systems. Dr. Arun Mangalam is the principal investigator and Dr. Martin Brenner is the NASA technical monitor. This work was also partially supported by NASA under Grant No. NRA NNX12AM55A entitled *Analytical Validation Tools for Safety Critical Systems Under Loss-of-Control Conditions*, Dr. C. Belcastro is the technical monitor.

The first author gratefully acknowledges the financial support from Zonta International through the 2013 Amelia Earhart Fellowship.

REFERENCES

[1] Lind, R. and Brenner, M., *Robust aeroservoelastic stability analysis*, Springer-Verlag, London, 1999.

[2] Benani, S., Van Staveren, J. W., Beuker, B., and Meijer, J. J., "Flutter analysis of an F-16A/B in heavy store configuration," *Journal of Aircraft*, Vol. 42, No. 6, 2005, pp. 1565-1574.

[3] Lind, R., "Flutter margins for multimode unstable couplings with associated flutter confidence," *Journal of Aircraft*, Vol. 46, No. 5, 2009, pp. 1563-1568.

[4] Baldelli, D. H., Zeng, J., Lind, R., and Harris, C., "Flutter-Prediction tool for flight-test-based aeroelastic parameter-varying models," *Journal of Guidance, Control and Dynamics*, Vol. 32, No. 1, 2009, pp. 158-171.

[5] Beranek, J., Nicolai, L., Buonanno, M., Burnett, E., Atkinson, C., Holm-Hansen, B. and Flick, P., "Conceptual design of a multi-utility aeroelastic demonstrator," *13th AIAA/ISSMO Multidisciplinary Analysis Optimization Conference*, Fort Worth, TX, 2010, pp. 2194-2208.

[6] Raghavan, B., "Flight dynamics and control of highly flexible flying wings," Ph.D. Dissertation, Aerospace and Ocean Enginnering Dept., Virginia Polytechnic Institute and State University, Blacksburg, VA, 2009.

[7] Patil, M. J. and Hodges, D. H., "Flight dynamics and control of highly flexible flying-wings," *Journal of Aircraft*, Vol. 43, No. 6, 2006, pp. 1790-1798.

[8] Nguyen, N., and Tuzcu, I., "Flight dynamics of flexible aircraft with aeroelastic and inertial force interactions," *AIAA Atmospheric Flight Mechanics Conference*, Chicago, IL, 2009.

[9] MSC/NASTRAN, Structural and Multidiscipline Finite Element Analysis, Software Package, Ver. 2012, MSC Software Corporation, Santa Ana, CA, 2012.

[10] FEMAP, Engineering Finite Element Analysis, Software Package, Ver. 10.3, Siemens PLM Software, Munich, Germany, 2012.

[11] ZAERO, Engineers Toolkit for Aeroelastic Solutions, Software Package, Ver. 8.5, ZONA Technology Inc.,Scottsdale, AZ, 2011.

[12] Ljung, L., *System Identification: Theory for the user*, Prentice Hall, Englewood Cliffs, New Jersey, 1987.

[13] Juang, J. N. and Pappa, R. S., "An eigensystem realization algorithm for modal parameter identification and model reduction," *Journal of Guidance, Control and Dynamics*, Vol. 8, No. 5, 1985, pp. 620-627.

[14] Caicedo, J. M., Dyke, S. J., and Johnson, E. A., "Natural Excitation Technique and Eigensystem Realization Algorithm for Phase I of the IASC-ASCE Benchmark Problem: Simulated Data," *Journal of Engineering Mechanics*, Vol. 130, No.1, 2004, pp. 49-60.

[15] Burnett, E., Atkinson, C., Beranek, J., Sibbitt, B., Holm-Hansen, B., and Nicolai, L., "NDOF Simulation model for flight control development with flight test correlation," *AIAA Modeling and Simulation Technologies Conference*, Toronto, Canada, 2010, pp. 7780-7794.

[16] Ewins, D. J., *Modal Testing: Theory and Practice*, Research Studies Press Ltd., England, 1984.

[17] Agilent 35670A, "Agilent 35670A Service Guide", Agilent Technologies, Inc., 2011.

[18] Agilent 35670A, "Agilent 35670A Operator's Guide", Agilent Technologies, Inc., 2010.

[19] MATLAB, Language of Technical Computing, Software Package, Ver. R2012a, The Mathworks Inc, Nattick, MA, 2012.

[20] Ljung, L., "System Identification Toolbox: User's Guide," Ver. 9.0 (Release 2014a), The Mathworks Inc, Nattick, MA, 2014.

[21] Schwarz, B. J., Richardson, M. H., "Experimental Modal Analysis," *CSI Reliability Week*, Orlando, Florida, 1999.

[22] Gade, S., Herlufsen, H. and Konstantin-Hansen, H., "How to determine the modal parameters of simple structures," *Sound and Vibration*, Vol. 36, No. 1, 2002, pp. 72-73.

[23] Henriksen, H. J., Troldorg, L., Nyegaard, P., Sonnenborg, T. O., Refsgaard, J. C., and Madsen, B., "Methodology for construction, calibration and validation of a national hydrological model for Denmark", *Journal of Hidrology*, Vol. 280, No.1, 2003, pp. 52-71.

[24] Vinnicombe, G., *Measuring the Robustness of Feedback Systems*, Ph.D Dissertation, University of Cambridge, UK, 1992.